Cross-bridge Scheme and Force per Cross-Bridge State in Skinned Rabbit Psoas Muscle Fibers

Masataka Kawai and Yan Zhao
Department of Anatomy, College of Medicine, University of Iowa, Iowa City, Iowa 52242 USA

ABSTRACT The rate and association constants (kinetic constants) which comprise a seven state cross-bridge scheme were deduced by sinusoidal analysis in chemically skinned rabbit psoas muscle fibers at 20°C, 200 mM ionic strength, and during maximal Ca^{2+} activation (pCa 4.54–4.82). The kinetic constants were then used to calculate the steady state probability of cross-bridges in each state as the function of MgATP, MgADP, and phosphate (P_i) concentrations. This calculation showed that 72% of avilable cross-bridges were (strongly) attached during our control activation (5 mM MgATP, 8 mM P_i), which agreed approximately with the stiffness ratio (active:rigor, 69 ± 3%); active stiffness was measured during the control activation, and rigor stiffness after an induction of the rigor state. By assuming that isometric tension is a linear combination of probabilities of cross-bridges in each state, and by measuring tension as the function of MgATP, MgADP, and P_i concentrations, we deduced the force associated with each cross-bridge state. Data from the osmotic compression of muscle fibers by dextran T500 were used to deduce the force associated with one of the cross-bridge states. Our results show that force is highest in the AM*ADP·P_i state (A = actin, M = myosin). Since the state which leads into the AM*ADP·P_i state is the weakly attached AM·ADP·P_i state, we confirm that the force development occurs on P_i isomerization (AM·ADP·P_i → AM*ADP·P_i). Our results also show that a minimal force change occurs with the release of P_i or MgADP, and that force declines gradually with ADP isomerization (AM*ADP → AM·ADP), ATP isomerization (AM^+ATP → AM*ATP), and with cross-bridge detachment. Force of the AM state agreed well with force measured after induction of the rigor state, indicating that the AM state is a close approximation of the rigor state. The stiffness results obtained as functions of MgATP, MgADP, and P_i concentrations were generally consistent with the cross-bridge scheme.

INTRODUCTION

Muscle contraction occurs as a result of the interaction between myosin cross-bridges and actin. One of the aims of our investigation on the mechanisms of contraction is to correlate the mechanical events with the biochemical events of the cross-bridge cycle (Kawai, 1982; Fortune et al., 1991). With biochemical techniques, contractile proteins are purified, and their interactions with the substrate (MgATP), products (MgADP, P_i = phosphate), and their analogs, are studied. These "solution" studies identified numerous intermediate states of actin-myosin substrate and the hydrolysis product complexes (Tonomura et al., 1969; Bagshaw and Trentham, 1974; Taylor, 1979; Stein et al., 1979; Eisenberg and Greene, 1980; Geeves et al., 1984). However, since force cannot be measured in purified proteins, it is not known how force changes after cross-bridges are attached. Consequently, discussion on the step that generates force has been limited to speculation based on the step that loses a large amount of free energy (White and Taylor, 1976; Taylor, 1979; Huxley, 1980; Hibberd et al., 1985).

To obtain a realistic picture of the mechanisms of contraction, it is desirable to study a muscle fiber to which one can apply mechanical and chemical perturbations at the same time. Mechanical perturbation is desirable because in muscle fibers there exist load limitations on the rate constants (Huxley, 1957; Huxley and Simmons, 1971). Consequently, a length change modifies the reaction rate constants of elementary steps, creating a transient instability in the cross-bridge cycle. This instability is sensed by tension time courses, called "tension transients" in response to step length changes (Huxley and Simmons, 1971; Heinl et al., 1974), or "exponential processes" in response to sinusoidal length changes (Machin and Pringle, 1960; Kawai and Brandt, 1980). In principle, the rate constants of these tension transients or exponential processes provide information on the elementary steps of the cross-bridge cycle. Thus, research in muscle fibers circumvents the shortfalls of solution studies. However, in intact preparations, because of the presence of the sarcolemma, chemical perturbations could not be applied. This limits the number of identifiable cross-bridge states, and a correlation between observed exponential processes and underlying elementary steps remains largely speculation. Experiments using skinned fibers (Natori, 1954), in which the sarcolemmal barrier is physically or functionally removed, may yield a more realistic picture of the contractile apparatus. Chemical perturbation is desirable because ions and molecules of experimental interest can be perfused to the vicinity of the contractile proteins, thus enabling parallel experiments to those performed in the solution studies.

According to the biochemical schemes of the cross-bridge cycle, however, there are many intermediate states which can be identified (Tonomura et al., 1969; Taylor, 1979; Eisenberg and Greene, 1980; Geeves et al., 1984). Questions are raised (Brenner, 1990) whether one can resolve such a complicated system in muscle fibers, deduce the necessary kinetic constants to characterize the system, and determine at which step force is generated. One method of approaching this problem

Received for publication 11 November 1992 and in final form 21 April 1993.
Address reprint requests to Dr. Kawai.

0006-3495/93/08/638/14 $2.00

is to use photolysis of "caged" compounds (Goldman et al., 1984a, 1984b; Dantzig et al., 1988, 1992; Millar and Homsher, 1990, 1992; Walker et al., 1992), which induces an increase in the concentration of a small ligand by a photochemical reaction, and to follow the time course of the tension change to identify the elementary steps. Although this method is conceptually simple and potentially useful, there can be technical difficulties with caged compounds such as nonspecific effects of caged P_i and caged ATP (Millar and Homsher, 1992) and the slow speed of photolysis of caged ATP (Goldman et al., 1984a).

Another approach is to use sinusoidal length perturbations of a small amplitude and monitor amplitude and phase shift in tension (Machin and Pringle, 1960; Kawai and Brandt, 1980). The small length perturbations presumably modify the rate constants of the elementary steps, and this modification in turn results in the transition between the cross-bridge states. Since some cross-bridge states support tension, while others do not, the transient instability in the cross-bridge cycle is detected as amplitude and phase shift in tension at each frequency. In sinusoidal analysis, it is approximately correct to state that any reaction faster than the frequency of oscillation appears to be at equilibrium, whereas any reaction slower than the frequency of oscillation appears not to happen (Hammes, 1968; Kawai and Halvorson, 1989, 1991). By selecting a particular frequency one can study a specific elementary step in the cross-bridge cycle. An additional advantage of sinusoidal analysis is that it is intrinsically a signal averaging procedure, hence the signal from the specific elementary step can be enhanced by increasing the duration of the measurement. With sinusoidal analysis, we have established a cross-bridge scheme based on six to seven states (Kawai and Halvorson, 1991; Zhao and Kawai, 1993), determined the kinetic constants which characterize the scheme, and discovered that tension is generated on cross-bridge attachment based on the P_i dependence of isometric tension. In this report, we have extended the analysis method, and determined the force associated with each cross-bridge state. Preliminary accounts of these results have been reported (Kawai and Zhao, 1992).

MATERIALS AND METHODS

Since experimental procedures were previously described (Kawai and Brandt, 1980; Zhao and Kawai, 1993), we only briefly outline the methods here. Experiments were performed at 20°C on small bundles (one to three fibers) of rabbit psoas muscle during maximal Ca^{2+} activation (pCa 4.54–4.82). The sarcomere length was adjusted to 2.5 μm by optical diffraction. The muscle length was changed sinusoidally with small amplitudes (±1.6 nm/cross-bridge), and tension amplitude and phase shift were detected (Machin and Pringle, 1960; Kawai and Brandt, 1980). Amplitude and phase shift were represented in the quantity called complex modulus $Y(f)$, where f is the frequency of length oscillation. The frequency range used in this report was 0.25–350 Hz. We have identified four exponential processes in the complex modulus of maximally activated rabbit psoas fibers (Zhao and Kawai, 1993):

$$\underset{\text{Process (A)}}{} \quad \underset{\text{Process (B)}}{} \quad \underset{\text{Process (C)}}{} \quad \underset{\text{Process (D)}}{}$$
$$Y(f) = H + A/(1 + a/fi) - B/(1 + b/fi) + C/(1 + c/fi) + D/(1 + d/fi) \quad (1)$$

$$Y_\infty \equiv H + A - B + C + D \quad (2)$$

We denote characteristic frequencies of respective processes by a, b, c, d, and their magnitudes by A, B, C, D. $i = -1$, and 2π times characteristic frequencies represent apparent (equals observed) rate constants. H is a constant that is small in fast twitch skeletal muscle fibers, and it is the modulus extrapolated to the zero frequency. Y_∞ is the modulus extrapolated to the infinite frequency, which is referred to as "stiffness" in our reports, and it is proportional to the number of attached cross-bridges. Y_∞ corresponds to phase 1, process (D) to the fast components of phase 2, process (C) to the slow component of phase 2, process (B) to phase 3, and process (A) to phase 4 of step analysis (Huxley and Simmons, 1971; Heinl et al., 1974). These correlations are summarized in Table 1. All exponential processes are absent when muscle fibers are relaxed (no Ca^{2+}) or brought into rigor (no MgATP), hence exponential processes are considered to reflect the dynamic interaction of cross-bridges with the thin filaments. Methods of obtaining the complex modulus data, the apparent rate constants, and the rate constants of elementary steps were described in earlier works (Kawai and Brandt, 1980; Kawai and Halvorson, 1989, 1991; Zhao and Kawai, 1993).

Compositions of solutions are summarized in Table 2. All activating solutions were prepared initially without CaEGTA. To activate the muscle preparation, 66 mM CaEGTA (pH 7.00) was added for the final concentration of 6 mM. We normally use 5 mM MgATP and 8 mM P_i for our experiments. This is because cross-bridges are more numerous in the AM^+S, AM*S, detached, and AM*DP states (see Scheme 1 for definition of these states), hence resolution of exponential processes (B), (C), and (D), which represent interconversions among these states, is better than in solutions that contain lower MgATP and/or P_i concentrations. The MgATP study was carried out in the range of 0.1 to 10 mM by mixing two solutions *0S* and *10S*, where *S* stands for the mM $MgATP^{2-}$ concentration. The P_i study was carried out by mixing solutions *0P* and *16P*, where *P* stands for the added mM phosphate concentration. The MgADP study was carried out by mixing solutions *0D* and *8D*, where *D* stands for the total millimolar MgADP concentration. pCa of activating solutions *A*, *0S*, *10S*, *0P*, and *16P* was 4.82; pCa of the activating solution *0D* was 4.54, *8D* was 4.64. The $MgATP^{2-}$ concentration of solutions *A*, *0D*, *8D*, *0P*, and *16P* was 5.0 mM. The free ATP (ATP^{3-} and ATP^{4-}) concentration of solutions *A*, *0S*, *10S*, *0P*, and *16P*

TABLE 1 Correlation between elementary steps of cross-bridge cycle and mechanical transients

Mechanisms	Elasticity	Step 1b	Step 2	Step 4	Step 6*
Sinusoidal analysis (Kawai and Brandt, 1980; Zhao and Kawai, 1993)	Y_∞	Process (D)	Process (C)	Process (B)	Process (A)
Step analysis (Heinl et al., 1974; Huxley and Simmons, 1971)	Phase I	Phase 2 (fast)	Phase 2 (slow)	Phase 3	Phase 4
Step analysis (Abbott and Steiger, 1977)	Phase 0	Phase 1	Phase 2	Phase 3	Phase 4
Pressure release (Fortune et al., 1991)				Phase 2	Phase 3
P_i transient (Dantzig et al., 1992)				Phase II	

Steps refer to the steps in cross-bridge Scheme 1.

* Step 6 probably does not correlate with the quantities listed, because Process (A) is very small (or absent) in insect flight muscles (Machin and Pringle, 1960), cardiac muscles (Saeki et al., 1991), and partially cross-linked fast twitch skeletal muscles (Tawada and Kawai, 1990).

TABLE 2 Solution compositions (total added concentrations in millimolar)

	EGTA	CaEGTA	MgATP	ATP	ADP	$MgPr_2$	KP_i	Na_2CP	CK	A_2P_5	KPr	NaPr	MOPS
R	6	-	2	5	-	-	8	-	-	-	48	62	10
W	-	-	0.5	-	-	-	8	-	-	-	102	75	10
Rg	-	-	-	-	-	-	8	-	-	-	103	76	10
A	-	6	5.3	4.7	-	-	8	15	160	-	35	28	10
OS	-	6	0	5	-	-	8	15	160	-	40	38	10
10S	-	6	10.6	4.4	-	-	8	15	160	-	30	18	10
OD	-	6	6.1	-	0	0.32	8	-	-	0.2	69	66	10
8D	-	6	6.1	-	8	3.5	8	-	-	0.2	48	54	10
OP	-	6	5.3	4.7	-	-	0	15	160	-	53	28	10
16P	-	6	5.3	4.7	-	-	16	15	160	-	16	28	10

R = relaxing solution, W = washing solution, Rg = rigor solution, A = control activating solution, EGTA = K_2H_2EGTA, CaEGTA = $K_2CaEGTA$, MgATP = Na_2MgATP, ATP = $Na_2K_{1.7}H_{0.3}ATP$, ADP = $Na_{1.5}H_{1.5}ADP$, KP_i = $K_{1.5}H_{1.5}PO_4$, Na_2CP = creatine phosphate, CK = creatine kinase (units/ml), A_2P_5 = P^1,P^5-di(adenosie-5′) pentaphosphate, Pr = propiontae, MOPS = morpholinopropane sulfonic acid.

was 5.0 mM. The Mg^{2+} concentration of solutions 0D and 8D was 1 mM. pH of all solutions was adjusted to 7.00, and ionic strength to 200 mM. For a series study which changed the ligand (MgATP, MgADP, or P_i) concentration, an approximately equal number of experiments was performed for the increasing and decreasing concentrations so that any artifact (if present) due to the order of experiments can be cancelled after averaging.

RESULTS

Cross-bridge scheme and the kinetic constants

To characterize elementary steps involved in the MgATP binding and subsequent reactions which ensue, we studied the effect of MgATP on the apparent rate constants (Fig. 1) (Zhao and Kawai, 1993). We found that the apparent rate constants $2\pi b$, $2\pi c$, and $2\pi d$ all increased with an increase in the MgATP concentration in the low mM range, and saturated in the high mM range. These results are consistent with the cross-bridge scheme that includes step 1a (MgATP binding), step 1b (ATP isomerization), step 2 (cross-bridge detachment), and step 4 (P_i isomerization) (Zhao and Kawai, 1993).

SCHEME 1

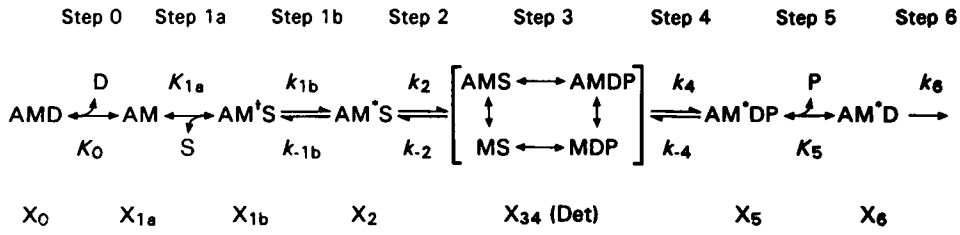

where A = actin, M = myosin head, S = substrate = MgATP, D = MgADP, and P = phosphate (P_i). *S*, *P*, and *D* indicate respective concentrations in algebraic expressions: $S = [MgATP^{2-}]$, $P = [P_i]_{total}$, $D = [MgADP^-]$. An asterisk (*) or a plus sign (+) identifies the second (and third) conformational state(s). Det (X_{34}) includes all detached states (MS, MDP) and weakly attached states (Stein et al., 1979; Greene and Eisenberg, 1980; Schoenberg, 1988; Brenner et al., 1991) (AMS, AMDP). These are combined and recognized as the lump sum detached state. In skinned fiber experiments at physiological ionic strength (200 mM), the weakly attached states represent only 1–2%, and the majority is in truly detached states, hence the name. Because of this nomenclature, we have named step 2 "detachment step," and step 4 "attachment step" to represent the behavior of the majority of the cross-bridges (Kawai and Halvorson, 1989, 1991; Zhao and Kawai, 1993). It is likely, however, that detachment and attachment steps occur via weakly attached states AMS and AMDP (Brenner et al., 1991), respectively. Because other investigators named step 4 "isomerization step" (Dantzig et al., 1992; Fortune et al., 1991; Walker et al., 1992), we use the same nomenclature in this report to avoid confusion. X_i (X_0, X_{1a}, . . . , X_6) in Scheme 1 indicates the steady-state probability of cross-bridges in the corresponding state. Table 1 summarizes elementary steps and their correlation with phases and processes observed in various techniques.

The MgATP effect (Fig. 1) is consistent with the assumption that the MgATP binding is faster than our observation speed (350 Hz, 2200 s^{-1}). If the binding is comparable to the observation speed, the plot would be linear; this is because the apparent rate constant is approximately the sum of the forward and backward rates, hence if we are observing a binding reaction directly, one of the rates is proportional to the MgATP concentration, therefore the apparent rate constant is linear to the MgATP concentration. This is apparently not the case in Fig. 1. The MgATP effect in Fig. 1 is also consistent with an assumption that step 1b is observed by process (D), step 2 by process (C), and step 4 by process (B) (Table 1). If the assignment of processes (C) and (D) were transposed, then a slower process (C) (hypothetical step 1b) would be interposed between step 1a (MgATP binding) and step 2, hence $2\pi d$ (hypothetical step 2) becomes insensitive to the MgATP

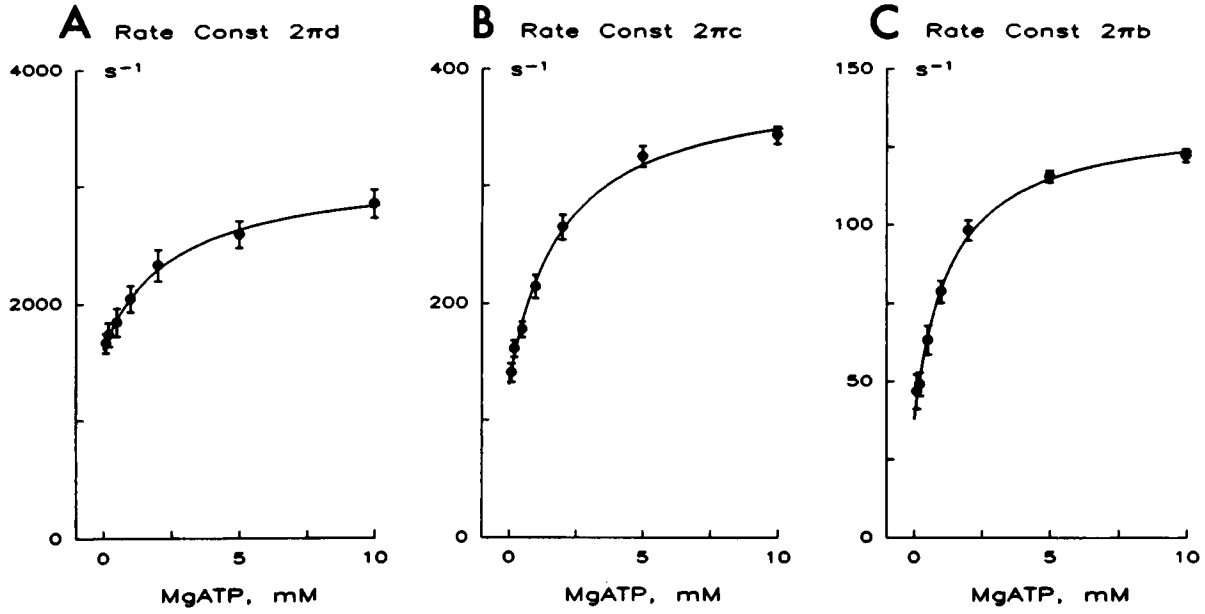

FIGURE 1 The apparent rate constants $2\pi d$ (in A), $2\pi c$ (in B), and $2\pi b$ (in C) are plotted as a function of the MgATP concentration. The continuous curves indicate hyperbolic fit to the respective rate constants. The abscissa refers to [$MgATP^{2-}$].

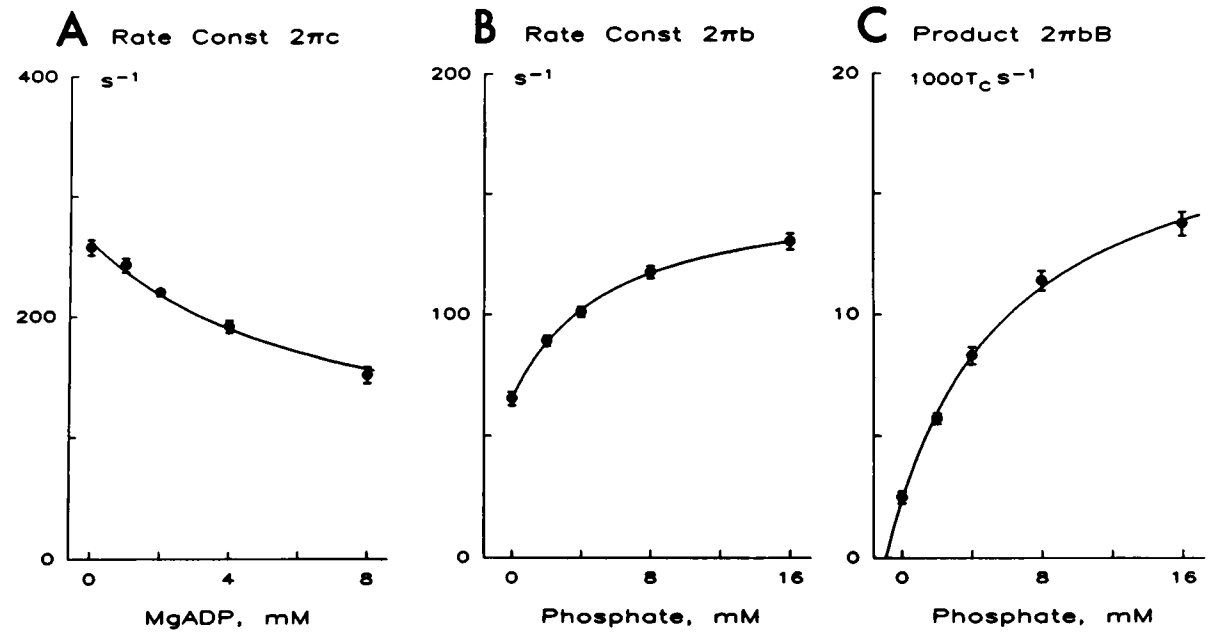

FIGURE 2 The apparent rate constant $2\pi c$ is plotted against the total MgADP concentration in A, the apparent rate constant $2\pi b$ is plotted against the added P_i concentration in B, and the product $2\pi b \cdot B$ is plotted against the added P_i concentration in C. The continuous curves indicate hyperbolic fit to the respective data.

concentration. This is contrary to our observation shown in Fig. 1 *A*. Similarly, the assignment of processes (B) and (C) could not be transposed, because then $2\pi c$ becomes insensitive to the MgATP concentration. The MgATP study yielded K_{1a} (0.23 ± 0.04 mM^{-1}), k_{1b} (1880 ± 220 s^{-1}), k_{-1b} (1510 ± 110 s^{-1}), K_{1b} (1.29 ± 0.15), k_2 (510 ± 30 s^{-1}), k_{-2} (132 ± 7 s^{-1}), and K_2 (3.9 ± 0.3) (Zhao and Kawai, 1993). These are the results of averaging 10 experiments (mean ± SE).

To characterize the elementary step involved in MgADP binding, the MgADP concentration was changed and its effect on the apparent rate constants was studied (Zhao and Kawai, 1993). It turned out that the effect was opposite to that of MgATP: all three rate constants $2\pi b$, $2\pi c$, and $2\pi d$, decreased with an increase in the MgADP concentration, and their plots were concave upward (Kawai and Halvorson, 1989; Zhao and Kawai, 1993). Fig. 2 *A* shows the rate constant $2\pi c$, and others were similar. To explain this re-

sult one must add a fast step 0 as shown in Scheme 1. This result is consistent with the hypothesis that MgADP is a competitive inhibitor of the substrate.[1] Once again, the fact that Fig. 2 *A* is curved rather than linear implies that the MgADP binding is faster than our observation speed. The MgADP experiment yielded K_0 (0.58 ± 0.09 mM^{-1}, N = 7) (Zhao and Kawai, 1993). It is evident that MgADP binds to myosin cross-bridges 2.5 × more strongly than MgATP.

To characterize the P_i binding step and P_i isomerization step, the P_i concentration was changed and its effect on the apparent rate constant $2\pi b$ was followed. When the P_i concentration was increased, $2\pi b$ increased and the plot was concave downward (Fig. 2 *B*). This implies that the P_i binding step is faster than our observation speed, otherwise the plot would be linear. This result is consistent with the scheme that adds P_i release step 5 as shown in Scheme 1. The result is also consistent with the assumption that step 4 is observed by process (B). The P_i study (N = 11) yielded k_4 (106 ± 4 s^{-1}), k_{-4} (90 ± 5 s^{-1}), K_4 (1.20 ± 0.07), and K_5 (0.19 ± 0.02 mM^{-1}) (Zhao and Kawai, 1993).

ATP hydrolysis takes place in step 3, while cross-bridges are detached from actin (MS → MDP) (Bagshaw and Trentham, 1974), or while cross-bridges are weakly attached to actin (AMS → AMDP) (Stein et al., 1979). Currently, all detached states (MS, MDP) and weakly attached states (AMS, AMDP) are combined and recognized as the lump sum detached state (Det). We know that step 3 cannot be much slower than $2\pi b$, otherwise $2\pi b$ becomes insensitive to MgATP concentration, which is contrary to our result (Fig. 1 *C*).

Step 6 is the slowest forward reaction in the cross-bridge cycle, i.e., step 6 limits the steady-state ATP hydrolysis rate. If it is a faster reaction, we could not explain the MgATP, MgADP, and P_i effects on three apparent rate constants.[2] Thus we call step 6 the rate-limiting step. At this time, it is not known whether step 6 results in the AMD state (ADP isomerization) or directly in the AM state (ADP desorption). However, the equilibrium of step 6 is expected to be much to the right (otherwise, hydrolysis cannot progress). For simplicity of argument, we assume that the AMD state is on the hydrolysis pathway, and that step 6 represents the ADP isomerization. In fact, Sleep and Hutton (Sleep and Hutton, 1980) observed two energetically different acto-S1·ADP states, and the equilibrium is 50–100 × toward the low energy state. Their low energy state corresponds to the AMD state, and their high energy state corresponds to the AM*D state in Scheme 1. The rate constant of step 6 was characterized by the ATP hydrolysis rate, which yielded k_6 to be 9–16 s^{-1} (Kawai and Halvorson, 1991; Zhao and Kawai, 1993).

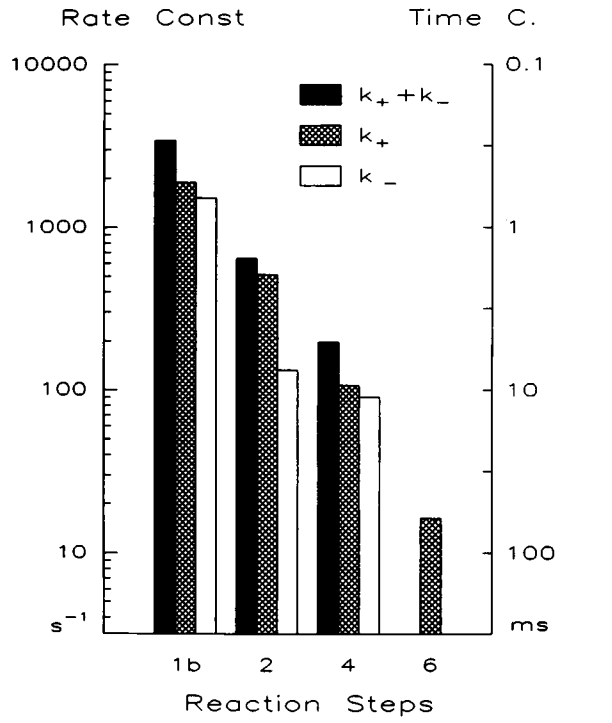

FIGURE 3 Rate constants of elementary steps (*left ordinate*) and corresponding time constants (*right ordinate*) are plotted. Forward reactions are shown in cross-hatched bars, backward reactions in white bars, and their summation in black bars. Steps 0, 1a, and 5 are faster than our speed of observation and are not included in the plot.

Scheme 1 is similar to that developed from solution studies (Taylor, 1979; Eisenberg and Greene, 1980; Geeves et al., 1984). Combining sinusoidal analysis in skinned fibers with the ATP hydrolysis rate measurement, we were able to determine all seven rate constants and three association constants needed to characterize Scheme 1. The rate constants of elementary steps are plotted in Fig. 3 in the log scale. As seen in Fig. 3, we found that the rate constants gradually decrease starting from step 1b and ending at step 6; an exception is step 5 (P_i release step), which is faster than the speed of our measuring apparatus and is not included in Fig. 3.

Magnitude *B*

The magnitude parameter B of process (B), in principle, is proportional to the number of cross-bridges in the AM*DP

[1] The theoretical curve in Fig. 2 *A* was derived based on the assumption that there is only one nucleotide binding site on the myosin head, and that this site can be occupied either by MgATP or MgADP under the present experimental conditions. Since MgADP is not hydrolyzed, the above condition qualifies MgADP to be a competitive inhibitor. The equation to describe the binding of MgADP was published in earlier papers (Eq. 3 (Kawai and Halvorson, 1989); Eq. 35 (Zhao and Kawai, 1993)).

[2] If step 6 is much faster than step 4, then $2\pi b$ represents step 6 rather than step 4. If this is so, one can predict that an increase in P_i concentration should diminish the apparent rate constants $2\pi b$, $2\pi c$, $2\pi d$; an increase in MgATP concentration should diminish $2\pi b$; and an increase in MgADP concentration should increase $2\pi b$. These predictions are altogether contradictory to our results (some of which are shown in Figs. 1 *C* and 2 *B*). See earlier papers (Kawai and Halvorson, 1989, 1991; Zhao and Kawai, 1993) for the discussion on the slowest forward reaction in the cross-bridge cycle.

state, hence B should diminish as the P_i concentration is reduced to 0. Since the analytical form of the product $2\pi b \cdot B$ is hyperbolic with respect to P and simpler than the magnitude itself (Kawai and Halvorson, 1991), the product is used for data fitting (Fig. 2 *C*).

$$2\pi b \cdot B = B_0 k_4 X_{34} = B_0 k_{-4} X_5 = B_0 k_{-4} K_5 P / [1 + \phi K_5 P] \quad (3)$$

where

$$\phi = \phi(S, D) = 1 + \frac{1 + K_0 D + K_{1a} S(1 + K_{1b} + K_{1b} K_2)}{K_{1a} S K_{1b} K_2 K_4}, \quad (4)$$

and B_0 is the proportionality constant that indicates the sensitivity of process (B) to the imposed length change. The steady-state probabilities X_{34} and X_5 are derived in Eqs. 23 and 24 (see Appendix). Actual fitting was performed on a modified form of Eq. 3, which replaced P with $P + P_0$, and the extra parameter P_0 also was deduced by the data fitting. This modification was necessary because the product data did not extrapolate to 0 when P_i was reduced to 0. As seen in Fig. 2 *C*, $2\pi b \cdot B$ decreased with a decrease in P_i concentration, and the plot extrapolated to 0 at a negative P_i concentration ($P = -1.0$ mM). This result implies that, in the absence of added P_i, about 1 mM P_i existed in the muscle fiber. There may be several reasons for this extra P_i: (i) continous liberation of P_i owing to hydrolysis of ATP in the muscle fiber, (ii) contamination of P_i mostly in creatine phosphate, and (iii) AM through AM*DP (X_{1a}–X_5) states are somewhat populated owing to the finite k_6 (instead of 0) even in the absence of P_i. These factors effectively displace the abscissa of Fig. 2 *C*. The value 1 mM is similar to an earlier report (0.6 mM (Kawai and Halvorson, 1991)). It also compares to the value 0.2 mM obtained using the sucrose and-sucrose phosphorylase system to reduce the endogenous P_i (Pate and Cook, 1989; Millar and Homsher, 1992).

Probability of cross-bridge states

We calculated the probability of cross-bridge states (Fig. 4), based on the kinetic constants thus deduced and Eqs. 19–26 (Appendix) which are based on Scheme 1. The probability is the same as the fractional concentration of the particular cross-bridge state. Evidently, the probability changes with the ligand concentrations S, P, and D, hence their dependence is plotted in Fig. 4. As seen in these plots all curves are hyperbolic; this is also evident in Eqs. 19–26. In Fig. 4 *C*, the abscissa is shifted by 1 mM to the right to account for the extra P_i (1.0 mM) which is present in the muscle fiber in the absence of exogenous P_i (see above). Under control activating conditions (S = 5 mM, P = 8 + 1 mM, pCa 4.8, CP/CK), the probabilities are found to be: AM (5%), AM^+S (6%), AM*S (7%), Det (28%), AM*DP (34%), AM*D (20%), and 72% of cross-bridges are (strongly) attached. The

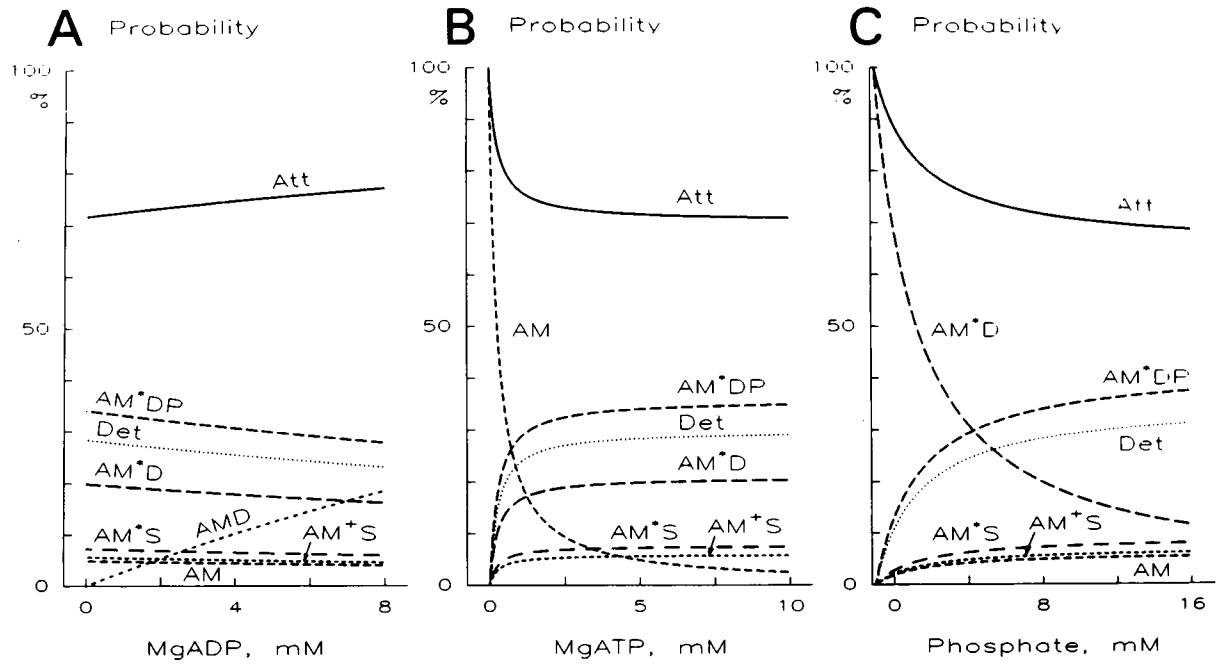

FIGURE 4 Steady-state probabilities of seven cross-bridge states are calculated from Eqs. 19–25 and plotted in percent as functions of MgADP (in *A*), MgATP (in *B*), and P_i (in *C*) concentrations. Also included are the summations of the probabilities of (strongly) attached states labeled *Att* (Eq. 26). The probability of the AMD state is not included in *B* and *C*, because it is less than 0.1%. In *C*, the abscissa is shifted by 1 mM to the left according to the results shown in Fig. 2 *C*. The kinetic constants used are: $K_0 = 0.58$ mM^{-1}, $K_{1a} = 0.23$ mM^{-1}, $K_{1b} = 1.29$, $K_2 = 3.9$, $K_4 = 1.20$, and $K_5 = 0.19$ mM^{-1} (Zhao and Kawai, 1993). Other than the variables in the abscissa, the parameters of the control conditions (S = 5 mM, D = 0.01 mM, P = 8 + 1 mM) are used.

probability for cross-bridges in the AMD state is less than 0.1%, because the estimated MgADP concentration is less than 20 μM (Meyer et al., 1985) in the presence of the ATP regenerating system CP/CK. Of the **Det** state, 1–2% is weakly attached, and the rest is in a truly detached state; this estimate is based on the rate constants measured at ionic strength 20 and 160 mM in resting rabbit psoas fibers at 5°C (Schoenberg, 1988), and an extrapolation to 200 mM by using the Debye-Hückel limiting law.

Tension per cross-bridge State

As indicated earlier, an additional advantage of our technique is that force is measured in the same activation as are the rate and equilibrium constants. Therefore, these kinetic constants can be readily utilized to construct a cross-bridge model, and the model's predictability of isometric tension can be examined by the actual tension measurement. One way of modeling isometric tension is a linear combination of the probabilities of cross-bridge states (Kawai and Zhao, 1992):

$$\text{Tension} = T_0X_0 + T_{1a}X_{1a} + T_{1b}X_{1b} + T_2X_2 + T_5X_5 + T_6X_6, \quad (5)$$

where X_i ($X_0, X_{1a}, \ldots, X_6$) represents the steady-state probability of the cross-bridges in respective state and as defined in Scheme 1, and T_i ($T_0, T_{1a}, \ldots, T_6$) is its linear coefficient: T_i indicates fiber tension if 100% of the cross-bridges are in state X_i, hence T_i is called "tension/cross-bridge state." We postulate that T_{34} is 0, because T_{34} is tension from detached or weakly attached cross-bridges. Eq. 5 assumes that cross-bridges in different states are arranged in parallel in the same half sarcomere so that their force is additive (cumulative).

Eq. 5 is rewritten into Eq. 6, based on the mass action law for step 1b (Eq. 14, Appendix), step 2 (Eq. 15), and step 4 (Eq. 16) as follows.

$$\text{Tension} = T_0X_0 + T_{1a}X_{1a} + T_xX_{1b} + T_6X_6, \quad (6)$$

where

$$T_x \equiv T_{1b} + K_{1b}T_2 + K_{1b}K_2K_4T_5. \quad (7)$$

We substituted X_i in Eq. 6 with analytical forms (Eqs. 19–21, 25), and performed linear regressions to obtain the coefficients T_i. Tension and stiffness data used in this section were collected at the same time as the rate constant results were collected (Zhao and Kawai, 1993), but were not published before. When the MgADP concentration (D) is increased, AMD (X_0) increases, whereas AM (X_{1a}), AM^+S (X_{1b}), and X_6 (AM*D) decrease proportionally (Fig. 4 *A*). Therefore, if linear fitting is performed to the results of isometric tension as the function of the MgADP concentration, the coefficient T_0 and a linear combination of T_{1a}, T_x, and T_6 ($T_{1a} + T_xK_{1a}S + T_6K_{1a}SK_{1b}K_2K_4/K_5P$) can be determined. Fig. 5 *A* represents averaged isometric tension plotted against the MgADP concentration and the best fit result based on Eq. 6. From this we obtained $T_0 = 1.31\ T_c$; T_i is expressed relative to T_c, which is the tension in the control activating solution (Table 3). Our observations of the effect of MgADP on isometric tension contrast to those of Cooke and Pate (1985) or Godt

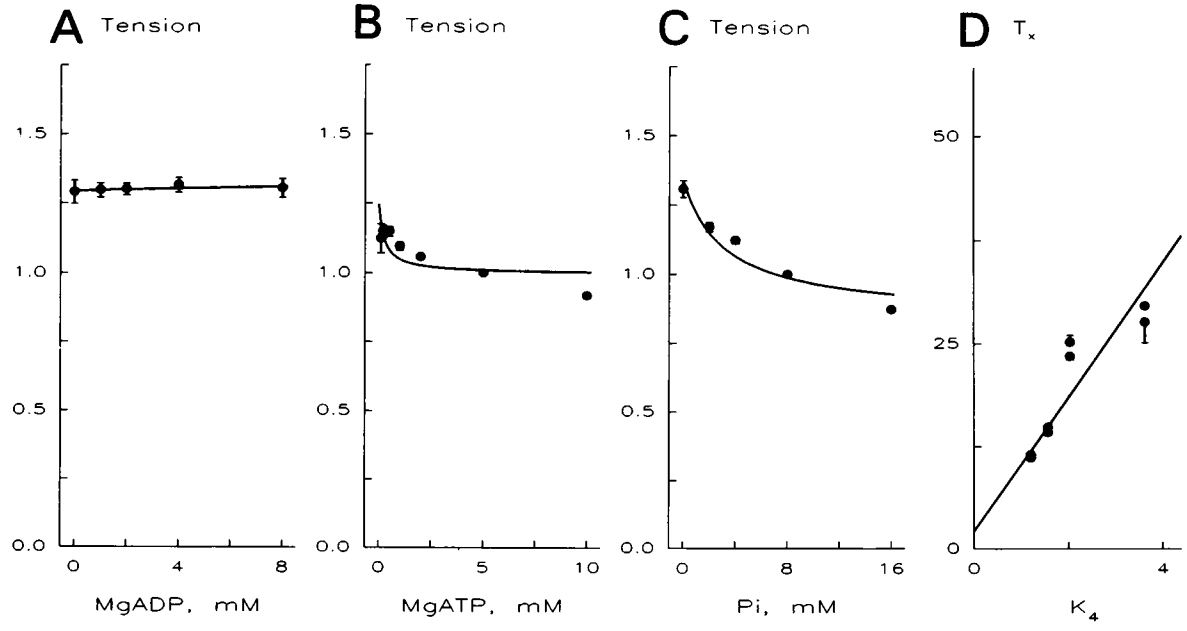

FIGURE 5 Isometric tension plotted as a function of the MgADP concentration ($N = 5$) in *A*, the MgATP concentration ($N = 12$) in *B*, and the P_i concentration ($N = 11$) in *C*. The data were first normalized to the value of control tension (T_c, Table 3), then averaged. Theoretical projections (*continuous lines*) are based on Eq. 6 and the kinetic constants obtained. *D*, T_x (defined in Eq. 7) is plotted against K_4 when fibers were compressed by dextran T500 (Zhao and Kawai, 1993). The averaged values are shown with mean ± SE error bars where appropriate; those smaller than symbol size are not seen. The units of all ordinates are T_c (tension in the control activating solution).

TABLE 3 Tension per cross-bridge state

Coefficient	State	Source	Average mean ± SE (N)	Units
T_0	AMD	ADP study	1.31 ± 0.12 (5)	T_c
T_{1a}	AM	ATP study	1.25 ± 0.06 (12)	T_c
T_{1b}	AM$^+$S	Estimate	1.25	T_c
T_2	AM*S	ATP/P_i studies	0.77	T_c
T_{34}	Det	Assumption	0	T_c
T_5	AM*DP	Dextran study	1.61	T_c
T_6	AM*D	P_i study	1.57 ± 0.05 (11)	T_c
T_c		ATP/P_i studies	240 ± 30 (22)	kN/m^2

T_c is tension in the control activating solution.

and Nosek (1989): they reported an increase in isometric tension as low mM MgADP was added to the activating saline. The reasons for the differences are not immediately clear.

When the MgATP concentration (S) is increased, AM (X_{1a}) decreases, whereas AM$^+$S (X_{1b}) and AM*D (X_6) increase (Fig. 4 B). X_0 (AMD) can be approximated by 0 (Eq. 19), because $K_0D < 0.012 \ll 1$ ($K_0 = 0.58$ mM^{-1}, $D < 0.02$ mM (Meyer et al., 1985)) in the presence of CP/CK. Therefore, if linear fitting is performed to the results of isometric tension as a function of the MgATP concentration (Eq. 6), the coefficient T_{1a} and a linear combination of T_x and T_6 ($T_x + T_6K_{1b}K_2K_4/K_5P$) can be obtained. Fig. 5 B represents averaged isometric tension plotted against the MgATP concentration, and the best fit result based on Eq. 6. From this we obtained $T_{1a} = 1.25\ T_c$.

When the P_i concentration (P) is increased, AM (X_{1a}) and AM$^+$S (X_{1b}) increase, whereas AM*D (X_6) decreases (Fig. 4 C). Therefore, if linear fitting is performed to the results of isometric tension as a function of the P_i concentration, the coefficient T_6 and a linear combination of T_{1a} and T_x ($T_{1a} + T_xK_{1a}S$) can be obtained. Fig. 5 C represents averaged isometric tension plotted against the P_i concentration, and the best fit result based on Eq. 6. From this we obtained $T_6 = 1.57\ T_c$. These results are summarized in Table 3, and entered in Fig. 6.

Because X_{1b} (AM$^+$S), X_2 (AM*S), and X_5 (AM*DP) have the same S, P, and D dependence (Eqs. 21, 22, 24; Fig. 4), their coefficients T_{1b}, T_2, and T_5 cannot be determined independently by studies that change MgATP, P_i, and MgADP concentrations. However, the MgATP and P_i studies determined T_x defined by Eq. 7. To determine T_{1b}, T_2, and T_5, some other method which changes probabilities X_{1b}, X_2, and X_5 independently is needed. When we carried out experiments that compressed muscle fibers with dextran T500, we found that K_0, K_{1a}, K_{1b}, and K_2 were not significantly affected by compression, whereas K_4 changed threefold (Zhao and Kawai, 1993). It then follows that if K_4 is increased, X_5 (AM*DP) increases (Eq. 24), whereas X_{1b} (AM$^+$S) and X_2 (AM*S) decrease (Eqs. 21 and 22). This property was used to determine T_5 based on Eq. 7 (see Fig. 5 D). From the slope of Fig. 5 D, we obtained $T_5 = 1.61\ T_c$; from the intercept, we obtained $T_{1b} + K_{1b}T_2 = 2.24\ T_c$.

Since there is no known way at this time to alter X_{1b} (AM$^+$S) and X_2 (AM*S) independently, there is no rational way to determine T_{1b} and T_2. Therefore, we have to make an estimate on T_{1b} and T_2. Because step 1b is seen in process (D), and process (D) is an exponential advance, $T_{1b} > T_2$ must hold. From this restriction and $K_{1b} = 1.29$, we obtain $2.24\ T_c > T_{1b} > 0.98\ T_c > T_2 > 0$. Furthermore, since AM$^+$S is a collision complex, the force in this cross-bridge (T_{1b}) may not be different from the force in the cross-bridge (T_{1a}) before the collision, AM. Such an example can be seen in step 5 (P_i release) and step 0 (MgADP release). Thus, if we assume $T_{1b} = T_{1a}$, then $T_{1b} = 1.25\ T_c$ and $T_2 = 0.77\ T_c$ will result. These values are entered in Table 3 and Fig. 6.

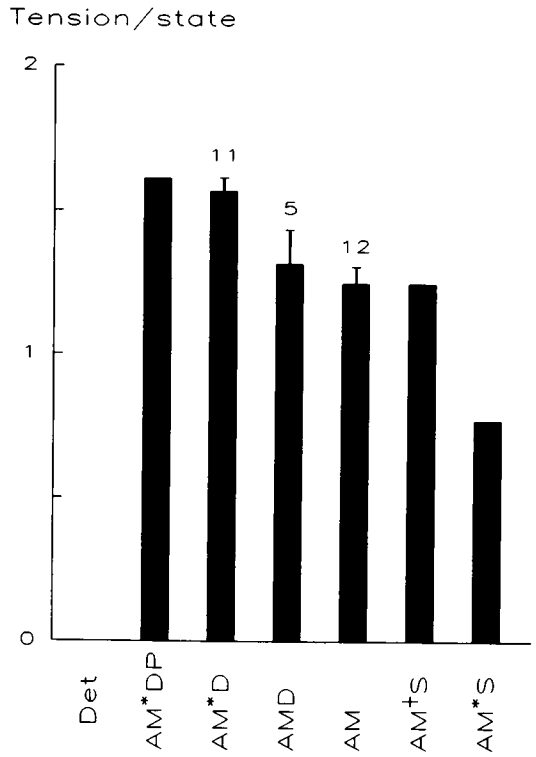

FIGURE 6 Tension/cross-bridge state is shown in T_c units. The amount of tension represents the tension value when all available cross-bridges are in the corresponding state. It is assumed that there is no tension in the Det state and that tension in the AM and AM$^+$S states is the same.

Stiffness (Y_∞) and the total number of attached cross-bridges

Stiffness (Y_∞ defined in Eq. 2) is proportional to the probability of (strongly) attached cross-bridges (X_{att}).

$$Y_\infty = Y_aX_{att} = Y_a(1 - K_{1a}SK_{1b}K_2K_5P/M), \qquad (8)$$

where Y_a is stiffness of the fiber when all cross-bridges are attached, X_{att} is given in Eq. 26, and M is defined in Eq. 27. The probability of attached cross-bridges is calculated and entered in Fig. 4 (labeled *Att*). Measured Y_∞ was plotted in Fig. 7 as functions of MgADP, MgATP, and P_i concentrations, and the data were fitted to Eq. 8. Theoretical projections based on Eq. 8 are denoted by continuous lines. As shown in Fig. 7, B and C, fitting was satisfactory for the

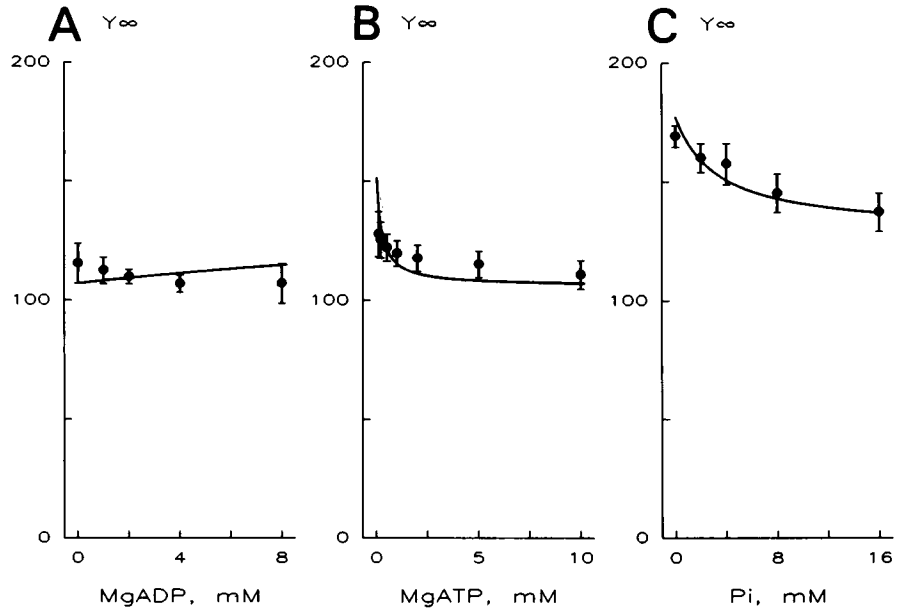

FIGURE 7 Stiffness (Y_∞) plotted as a function of the MgADP concentration (N = 5) in *A*, the MgATP concentration (N = 12) in *B*, and the P_i concentration (N = 11) in *C*. The stiffness data were first normalized to the value of control tension (T_c) of the same preparation, then averaged. Theoretical projections (*continuous lines*) are based on Eq. 8 and the kinetic constants obtained. The units of all ordinates are T_c (tension in the control activating solution).

MgATP and P_i study, and we obtained Y_a = 152 ± 6 (N = 12) for the MgATP study, and Y_a = 200 ± 8 (N = 11) for the P_i study. Fitting was less satisfactory for the MgADP study, although the theoretical projection is within the standard error of the means (Fig. 7 *A*), and we obtained Y_a = 150 ± 3 (N = 5). This may relate to the fact that the MgADP study is the most difficult of the three studies, because of faster deterioration of preparations in a solution that contained ADP (Kawai and Halvorson, 1989) than in a solution that contained CP/CK.

Comparison with the rigor state

To measure stiffness and tension of the fibers directly when all cross-bridges are attached, the preparation was activated with the control activating solution, followed by induction of the "high-rigor state" (Kawai and Brandt, 1976) by two full volume changes with the Rg solution (Fig. 8). One volume change was not adequate to induce rigor as judged by $Y(f)$, and three volume changes caused a decline of rigor tension presumably because of stretching of the fiber during the solution change, while rigor was partially induced. During the control activation, the complex modulus data $Y(f)$ were collected (Record 4, Fig. 8) and T_c was measured. $Y(f)$ was fitted to Eq. 1, and Y_∞ was deduced from Eq. 2. After rigor tension was developed in about 0.5 min, 40 mM EDTA was added for the final concentration of 3.6 mM to remove remaining magnesium so that trace MgATP concentration was reduced. Rigor tension slowly declined as seen in Fig. 8. The complex modulus data collected after rigor induction (records 6, 8, and 10 in Fig. 8) were almost independent of the frequency, and similar to those published earlier (Kawai and Brandt, 1980; Kawai, 1982). Thus, we used the modulus at 100 Hz for stiffness of the rigor state (Y_{rig}) that was collected at about 1.5 min after the rigor induction. Tension and stiffness values are expressed in terms of T_c and averaged. The results are summarized in Table 4.

The averaged rigor tension was T_{rig} = 1.28 ± 0.06 T_c (N = 8), and this agrees well with T_{1a} (1.25 ± 0.06 T_c, Table 3) of the AM state. The averaged rigor stiffness was Y_{rig} = 134 ± 12 T_c (N = 8), and it turned out to be lower than Y_a. Finally, Y_∞ during control activation was divided by Y_{rig} and averaged (Table 4). The result was: Y_∞/Y_{rig} = 69 ± 3 % (N = 8). This value represents the fraction of attached cross-bridges during the control activation. The fraction turned out to be a close match with the expectation (72%), based on the probability calculation (above) of the attached cross-bridges during the control activation.

DISCUSSION

We derived cross-bridge Scheme 1 and deduced the necessary kinetic constants to characterize Scheme 1 based on sinusoidal analysis on skinned psoas muscle fibers. These deductions are the results of the analysis of the MgATP, MgADP, and P_i effects on the apparent rate constants $2\pi b$, $2\pi c$, and $2\pi d$. Scheme 1 uniquely explains our data, and no other scheme with the same degree of simplicity explains the data. The cross-bridge Scheme 1 is comparable to (Kawai and Halvorson, 1991) or the same as (Zhao and Kawai, 1993) earlier reports; its partial scheme including the AMDP, AM*DP, and AM*D states (steps 4 and 5) is consistent with that derived from pressure-release experiment (Fortune et al., 1991) or photolysis of caged P_i (Dantzig et al., 1992; Walker et al., 1992) on rabbit psoas fibers. Scheme 1 is also comparable to that derived from solution studies of extracted protein systems (Tonomura et al., 1969; Taylor, 1979; Eisenberg and Greene, 1980; Geeves et al., 1984).

In pressure-release experiments, Fortune et al. (1991) observed two exponential time courses which they named phases 2 and 3. Their phase 2 corresponds to process (B), and phase 3 to process (A) of sinusoidal analysis (Table 1), based on the P_i sensitivity and the size of respective rate constants. They found that, as the P_i concentration was increased, the

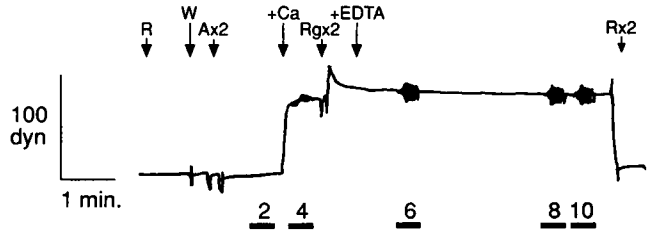

FIGURE 8 Slow tension time course of a preparation of three fibers. The preparation was initially soaked in the relaxing solution (*R*), which was replaced with the washing solution (*W*), and replaced twice with the control activating solution (A × 2) without CaEGTA. At +Ca, 66 mM CaEGTA was added (1:10 by volume). The solution was replaced twice with the rigor solution (Rg × 2), and 40 mM EDTA was added (1:10) at +EDTA. This solution was replaced twice with the relaxing solution (R × 2). Computer records were collected as indicated in the lower part of the figure, and as can be seen as oscillations in the tension trace. The figure was photographically reproduced from the original pen trace.

TABLE 4 Comparison of parameters of rigor and the control activation

	Average mean ± SE (*N*)	Units
T_{rig}	1.28 ± 0.06 (8)	T_c
Y_{rig}	134 ± 12 (8)	T_c
Y_∞/Y_{rig}	69 ± 3 (8)	%

Rigor state was induced from the control activation as described (Kawai and Brandt, 1976). Rigor tension (T_{rig}) and stiffness (Y_{rig}) were measured at about 1.5 min after induction of rigor, and these are expressed in terms of tension of the control activation (T_c). The ratio of Y_∞ of the control activation to $Y_{rig}$is shown in percent.

"reciprocal time constant" (= apparent rate constant) of phase 2 increased and saturated (see their Fig. 4 *A*) just as in Fig. 2 *B* of the present report. From this, they concluded that P_i release takes place in two steps, a result consistent with our earlier report (Kawai and Halvorson, 1991). Their rate constant was smaller, because their experiments were conducted at 12°C.

In caged-P_i experiments (Dantzig et al., 1992; Millar and Homsher, 1992; Walker et al., 1992), a small concentration (≤ 2.5 mM) of P_i was photochemically released, and the resulting tension transient was monitored. These studies (Dantzig et al., 1992; Millar and Homsher, 1992) observed a short lag (phase I) followed by an exponential decline of tension (phase II). Since the apparent rate constant of phase II was P_i-dependent, and it was concave downward when plotted against the P_i concentration, Walker et al. (1992) and Dantzig et al. (1992) concluded that P_i release takes place in two steps (steps 4 and 5 in Scheme 1), confirming the presence of the AM*DP state. These conclusions with caged P_i experiments are once again consistent with an earlier conclusion (Kawai and Halvorson, 1991). In fact, the current Fig. 2 *B* is very similar to Fig. 2 (Kawai and Halvorson, 1991), Fig. 3 (Walker et al., 1992), and Fig. 6 (Dantzig et al., 1992) of earlier works with respect to the P_i dependence and the range of the rate constant. The data presented in these figures are essential for the identification of the AM*DP state. Another report (Millar and Homsher, 1990) with the caged-P_i study included the state equivalent to the AM*DP state in their cross-bridge scheme; however, the presence of this state was not supported by experimental data, and the report did not establish the existence of the AM*DP state; their proof came later (Dantzig et al., 1992). We previously designated step 4 as the "cross-bridge attachment" step (Kawai and Halvorson, 1991; Zhao and Kawai, 1993), because the state which leads into step 4 is the combined Det state, most of which is occupied by the truly detached state(s). Other researchers (Fortune et al., 1991; Dantzig et al., 1992; Walker et al., 1992) designated step 4 as the isomerization step, because the reversal of step 4 results in the weakly attached state AMDP; the AMDP state rapidly detaches to form the MDP state at physiological ionic strength (Schoenberg, 1988). Thus, there is no substantial difference in conclusions derived from sinusoidal analysis, pressure-release experiment, and caged-P_i experiments. The correlation between the elementary steps of the cross-bridge cycle and processes and phases of various analysis techniques are listed in Table 2.

The forward rate constant of step 4 (k_4) was measured to be 106 s^{-1} in this report, which compares to 56 s^{-1} (Kawai and Halvorson, 1991), 79.2 s^{-1} (Dantzig et al., 1992) of earlier works at 20°C, and to 27 s^{-1} (Walker et al., 1992) at 15°C; all of these measurements were carried out on rabbit psoas fibers. A pressure-release experiment (Fortune et al., 1991) was carried out at 12°C on psoas, and the rate constant corresponding to k_4 was estimated to be 36 s^{-1}, and that corresponding to k_{-4} was estimated to be 15 s^{-1} from their Fig. 4 *A*. When we duduced k_4, a correction (a factor of 1.2) was applied based on the preceding step 2 (Kawai and Halvorson, 1991), whereas results from caged-P_i experiments did not include this correction. The backward rate constant of step 4 (k_{-4}) was measured to be 90 s^{-1}, which compares to 129 s^{-1} (Kawai and Halvorson, 1991), 115 s^{-1} (Walker et al., 1992), and 114.7 s^{-1} (Dantzig et al., 1992) of earlier works. The dissociation constant ($1/K_5$) of P_i was measured to be 5.3 mM, which compares to 14 mM (Kawai and Halvorson, 1991), 3.9 mM (Fortune et al., 1991), 6.1 mM (Walker et al., 1992), and 3.7 mM (Dantzig et al., 1992) of earlier works. Thus, a very good agreement of these kinetic constants is seen between the results of sinusoidal analysis, pressure-release, and caged-P_i experiments. Values in this report vary somewhat from our earlier report (Kawai and Halvorson, 1991) because of the difference in the analysis method: four exponential processes are used in this report instead of three (Kawai and Halvorson, 1991), and $2\pi b$ was independently fitted in this report (Fig. 2 *B*), whereas $2\pi b$ and $2\pi b \cdot B$ were fitted simultaneously in the earlier report (Kawai and Halvorson, 1991). In pressure-release and caged-P_i studies, only the apparent rate constant was used to fit the results, and the magnitude (amplitude) parameter was not used for the data analysis.

Our earlier report (Kawai and Halvorson, 1991) concluded that tension was generated at step 4. This conclusion was

based on the fact that the P_i dependence of the isometric tension can be explained if tension was supported by the AM*DP state, but the P_i dependence could not be explained if the tension was not supported by the AM*DP state. We have extended the analysis method, and deduced the tension supported by each cross-bridge state by assuming that isometric tension is a linear combination of the probabilities of cross-bridges in attached states (Eq. 5). The probability of cross-bridges was obtained from the kinetic constants as described in the Appendix. We found that T_5 of the AM*DP state is the highest tension of all attached states (Table 3 and Fig. 6), therefore, force generation must occur on P_i isomerization (step 4) as previously reported (Kawai and Halvorson, 1991). This conclusion is identical to that based on caged P_i experiments (Dantzig et al., 1992; Walker et al., 1992) published more recently. Dantzig et al. (1992) observed a 1–2-ms lag in phase I which presumably corresponded to the P_i-binding step where no tension change occurred, hence they concluded that tension supported before and after the P_i binding was the same; Walker et al. (1992) derived a similar conclusion without observing the lag phase. In fact, the continuity of their tension trace before and after the photorelease of P_i through the P_i transient demonstrates that the force supported by AM*D and AM*DP states is the same. If the force is different between the two states, an abrupt transition in the tension trace must be seen with the binding of P_i, an event which would be faster than the speed of observation. Based on both sinusoidal analysis and caged-P_i experiments, we conclude that force is generated by the P_i isomerization (step 4), and not by P_i release (step 5).

In solution studies, AM*DP was not recognized, and steps 4 and 5 were presumably combined and referred to as the "P_i-release step." The P_i binding in solution is very weak, and the dissociation constant was reported to be 10–100 M (Taylor, 1979). Thus, the P_i release step is practically irreversible in solution. In fiber studies in contrast, it has been known for some time that the P_i-release step is reversible by using isotope ^{32}P (Gillis and Maréchal, 1974; Mannherz, 1970; Ulbrich and Rüegg, 1971) and ^{18}O (Hibberd et al., 1985) exchange. This fact implies the potential energy represented by force in fibers can be transduced back to chemical energy. This is because the free energy of hydrolysis is retained as the potential energy and stretches the compliant portion of cross-bridges (or structures in series with them). Thus, it can be concluded that the total free energy change associated with step 4 is the sum of the free energy change measured by K_4 ($-RT \ln K_4$) and the potential energy evolution measured by force generation (Kawai and Halvorson, 1991).

Our results (Fig. 6) demonstrate that force is almost the same in the AM*DP and AM*D states, then declines with ADP isomerization (step 6) to the AMD state. Force in the AM state is similar to that in the AMD state. Furthermore, it is interesting to point out in Fig. 6 that force does not change significantly with the collision complex formation between a macromolecule (myosin cross-bridge) and small ligands (MgADP, P_i). This phenomenon is observed on the reversal of steps 0 and 5. This is reasonable, because force would be a result of the macromolecular architecture of the contractile apparatus, and addition or deletion of small ligands may not influence the architecture. If we apply the same reasoning to step 1a, then it follows that force in AM and AM^+S is the same ($T_{1a} = T_{1b}$). We then find that the force drops to about half in step 1b ($AM^+S \rightarrow AM^*S$). This result is reasonable because AM*S is a transient intermediate state that is followed by the detachment of cross-bridges in step 2. The gradual force decline in steps 1b and 2 is consistent with the fact that both process (D) (step 1b) and process (C) (step 2) are observed as exponential advances (positive terms in Eq. 1). Thus, we can generalize that force changes on isomerization after a collision complex formation, which occurs in step 1b ($AM^+S \rightarrow AM^*S$) and step 2 ($AM^*S \rightarrow AMS$); it also occurs in the reversal of step 4 ($AM^*DP \rightarrow AMDP$) and step 6 ($AMD \rightarrow AM^*D$). If we correlate the binding/release of substrate or products to a chemical step and the isomerization/conformational change to a mechanical step, then the above observation is comparable to A. F. Huxley's assertion (1980) that chemical and mechanical steps alternate in the cross-bridge cycle.

It is also interesting to observe that force per cross-bridge state is highest after the cross-bridge attachement, and force gradually declines while cross-bridges are attached to actin. We infer from this observation that force generation takes place only at a single step in the cross-bridge cycle, and no multiple force generation steps exist under our experimental conditions. If the muscle is allowed to shorten, then contraction would occur resulting in further decline of force. Alternatively, the gradual decline of force may imply that an attached cross-bridge slips to the next available actin site caused by rapid detachment and reattachment transitions (Brenner, 1990). This mechanism is more difficult to envision, however, because force (hence potential energy) on the cross-bridge is lost by cross-bridge detachment.

Our results (Fig. 6) demonstrate that no strongly attached, low force state (Cecchi et al., 1982) exists between the detached state Det (or weakly attached state AMDP) and the high force state AM*DP in fibers maximally activated with Ca^{2+}. Dantzig et al. (1988) by using adenosine 5′-*O*-(thio)-triphosphate (ATP(γS)) observed a cross-bridge state with large stiffness, but without tension, and suggested its significance in force generation. They reported that this cross-bridge state is different from the weakly attached state (AMS and AMDP in Scheme 1), because of its Ca^{2+} sensitivity and the slower detachment rate than in the weakly attached state. The cross-bridge state with ATP(γS) may correspond to the strongly attached AM*DP state but without tension. This inference is based on the fact that, in cross-bridge Scheme 1, the AM*DP state exists only in the presence of Ca^{2+}, whereas the weakly attached AMDP state was reported to exist with/without Ca^{2+} (Schoenberg, 1988; Brenner et al., 1991), hence step 4 must be regulated by Ca^{2+}. In our experiments, we did not observe a strongly attached low force state, presumably because the formation of AM*DP and force generation is simultaneous when ATP is used as the substrate. Although ATP(γS) is reported to be hydrolyzed

both by myosin subfragment one (S1) (Bagshaw et al., 1972) and acto-S1 (Goody and Mannherz, 1975), it appears that the hydrolysis energy of ATP(γS) cannot be utilized for force generation (Dantzig et al., 1988). An alternative possibility that ATP(γS) corresponds to the AM*S state is less likely, because of the Ca^{2+} sensitivity of stiffness associated with the ATP(γS) state (Dantzig et al., 1988); there is hitherto no known evidence that steps 1b or 2 (or their reversal) is controlled by Ca^{2+}.

The presence of the AM state during the cross-bridge cycle was assumed from earlier muscle research (Tonomura et al., 1969), and the AM state was designated as the "rigorlike state" (Lymn and Taylor, 1971) because this state did not have ATP or ADP molecules; hence, it was equivalent to the state in which ATP was depleted. However, it was never shown experimentally that the AM state and the rigor state were the same state. To prove this point, we induced the "high rigor" state (Kawai and Brandt, 1976) starting from the control activation, and rigor tension ($T_{rig} = 1.28 \pm 0.06\ T_c$) and stiffness ($Y_{rig} = 134 \pm 12\ T_c$) were measured (Fig. 8; Table 4). These values were compared with tension of the AM state ($T_{1a} = 1.25\ T_c$) and stiffness ($Y_a = 150$–$200\ T_c$) of attached cross-bridges during full activation in the presence of Ca, MgATP, and P_i. As this comparison demonstrates, a very good agreement was seen between T_{1a} and T_{rig}. An approximate agreement of Y_a and Y_{rig} was seen in MgATP and MgADP studies. Based on these results, we conclude that the AM state during full activation is a close approximation of the rigor state thus induced. We also examined the ratio Y_∞ during control activation to Y_{rig} (Table 4). This ratio ($69 \pm 3\%$) represents the number of (strongly) attached cross-bridges during the control activation, which is calculated to be 72% based on Eq. 26 and the kinetic constants deduced. Thus, a close agreement was obtained between the predicted value and the value based on the stiffness measurement, implying the appropriateness of the kinetic constants deduced.

Fig. 3 plots in the log scale the rate constants of elementary steps. This figure demonstrates that the reaction becomes progressively slower in each step. The only exception is the P_i release step 5, which is faster than our observation speed and not included in the figure. It appears from this figure that one purpose of the chemomechanical transduction is to achieve a slower speed. A chemical reaction would occur in the order of 1 ms, but this is too fast to generate any useful work. A slower speed is essential to result in sizable work generation. To understand this circumstance, it is necessary to introduce the quantity called "force-time product."

$$\text{Force-time product} = F \cdot \delta t = m \cdot V, \qquad (9)$$

where F is the force, δt is the duration (time) of the force application, m is the mass of the material being moved, and V is the velocity. The force-time product directly translates into the momentum ($m \cdot V$) by Eq. 9 to result in the shortening of the muscle. The kinetic energy transfered at this time is $F \cdot \delta y$ in the usual way, where δy is the distance shortened. Both the momentum and the kinetic energy must be generated to move an object. Step 6 is the most likely step to contribute to the force-time product, because it is the slowest step in the cross-bridge cycle, hence δt is largest. Steps 1b and 2 are not likely to contribute to the force product much, because these reactions are fast (Fig. 3). Thus, we conclude that much work is performed at step 6.

The AM^+S state is comparable to the collision complex reported in solution studies (Trybus and Taylor, 1982; Geeves et al., 1984), and the AM*S state is comparable to the reaction intermediate AM·ATP reported by White and Taylor (1976). In caged-ATP experiments (Goldman et al., 1984b), in which a small concentration (<2 mM) of ATP was photochemically released, intermediate states AM^+S and AM*S were not identified, presumably because of the slow sequential reactions of the photo-release of ATP (64 and 118 s^{-1} (Goldman et al., 1984a)). We believe that the primary site of the perturbation by the length change is either the nucleotide binding (step 1a) or subsequent isomerization (step 1b) to cause characteristic tension transients. In fact, Kuhn and others (Kuhn, 1977; Marston et al., 1979) presented evidence in insect muscles that the nucleotide binding step is influenced by the imposed length change using adenosine 5′-(β,γ-imidotriphosphate) (AMP-PNP). With sinusoidal analysis in skinned psoas fibers, the MgATP association constant was measured at 0.23 mM^{-1}, the rate constants of the forward and reversal of the ATP isomerization step were measured at 1880 and 1510 s^{-1}, respectively, and the rate constants of the forward and reversal of the cross-bridge detachment step were measured at 510 and 132 s^{-1}, respectively (Kawai, 1982; Kawai and Halvorson, 1989; Zhao and Kawai, 1993).

Our finding, that a single force value is associated with a cross-bridge state, can be explained in terms of distributed cross-bridge strain (Huxley, 1957; Huxley and Simmons, 1971). The measured force per cross-bridge state (T_i) is the average force over the distributed strain in the same cross-bridge state:

$$T_i = \int_I EyX_i(y)\,dy \Big/ \int_I X_i(y)\,dy = E\bar{y}_i, \qquad (10)$$

where E is the Young's elastic modulus of the muscle fiber (or stiffness of a cross-bridge after proper scaling), $X_i(y)$ is the strain distribution of the cross-bridges in the state X_i, and y is the strain on a cross-bridge. $\bar{y}_i$ is the averaged strain over $X_i(y)$:

$$\bar{y}_i \equiv \int_I X_i(y)y\,dy \Big/ \int_I X_i(y)\,dy \qquad (11)$$

Definite integrals (I) represent the entire domain of the strain distribution, normally from $-\infty$ to $+\infty$. The integrals in the denominator are present, because the individual value $X_i(y)$ is not normalized (Eq. 18).

Because in general a rate constant of an elementary step is strain-sensitive $\{k_i = k_i(y)\}$, it might be considered that no single value may be assigned to the rate constant. Our results are not in contradiction to this general idea: k_i corresponds to the value at $\bar{y}_i$, that is $k_i = k_i(\bar{y}_i)$.

In conclusion, we confirmed that force is generated at step 4 and before P_i is released. Step 6 is the rate-limiting step which occurs after the P_i release; cross-bridges are in the AM*D state long enough that work is performed at this step. We found that force per cross-bridge state changes little with the binding/release of small ligands (MgATP, MgADP, P_i), possibly because force is the result of macromolecular architecture. We found that the force change occurs with the isomerization (conformational change) which follows the binding/release of the ligands; we also found that force gradually decreases with subsequent conformational changes during which cross-bridges are attached. Thus, our approach yielded new insights into the cross-bridge mechanisms of contraction in skeletal muscle fibers.

APPENDIX

In the following analysis, X_i represents the steady-state probability of cross-bridges in the respective state as shown in Scheme 1. The steady-state probability can be obtained by assuming the mass action law as an approximation for steps 0–5. The mass action law cannot be applied to the rate-limiting step 6.

$$X_{1a} = X_0/K_0D \quad \text{(Step 0)} \tag{12}$$

$$X_{1b} = X_{1a}K_{1a}S \quad \text{(Step 1a)} \tag{13}$$

$$X_2 = X_{1b}K_{1b} \quad \text{(Step 1b)} \tag{14}$$

$$X_{34} = X_2K_2 \quad \text{(Step 2)} \tag{15}$$

$$X_5 = X_{34}K_4 \quad \text{(Step 4)} \tag{16}$$

$$X_6 = X_5/K_5P \quad \text{(Step 5)} \tag{17}$$

In addition, since the values of X_i are probabilities (conservation rule)

$$X_o + X_{1a} + X_{1b} + X_2 + X_{34} + X_5 + X_6 \equiv 1 \tag{18}$$

From Eqs. 12–18, we obtain:

$$X_0 = K_0DK_5P/M \quad \text{(AMD)} \tag{19}$$

$$X_{1a} = K_5P/M \quad \text{(AM)} \tag{20}$$

$$X_{1b} = K_{1a}SK_5P/M \quad \text{(AM}^+\text{S)} \tag{21}$$

$$X_2 = K_{1a}SK_{1b}K_5P/M \quad \text{(AM*S)} \tag{22}$$

$$X_{34} = K_{1a}SK_{1b}K_2K_5P/M \quad \text{(Det)} \tag{23}$$

$$X_5 = K_{1a}SK_{1b}K_2K_4K_5P/M \quad \text{(AM*DP)} \tag{24}$$

$$X_6 = K_{1a}SK_{1b}K_2K_4/M \quad \text{(AM*D)} \tag{25}$$

$$X_{att} \equiv X_0 + X_{1a} + X_{1b} + X_2 + X_5 + X_6 = 1 - X_{34} = 1 - K_{1a}SK_{1b}K_2K_5P/M \tag{26}$$

where

$$M \equiv K_{1a}SK_{1b}K_2K_4 + K_5P[1 + K_0D + K_{1a}S(1 + K_{1b} + K_{1b}K_2 + K_{1b}K_2K_4)] \tag{27}$$

Note that M is linear to S, P, or D, and positively correlated. Eqs. 19–26 are plotted in Fig. 4.

This work was supported by grants from the National Science Foundation (DCB90-18096) and the Iowa Affiliate of the American Heart Association (IA-91-G-13).

REFERENCES

Abbott, R. H., and G. J. Steiger. 1977. Temperature and amplitude dependence of tension transients in glycerinated skeletal and insect fibrillar muscle. *J. Physiol. (Lond.).* 266:13–42.

Bagshaw, C. R., and D. R. Trentham. 1974. The characterization of myosin-product complexes and of product-release steps during the magnesium ion-dependent adenosine triphosphatase reaction. *Biochem. J.* 141: 331–349.

Bagshaw, C. R., J. F. Eccleston, D. R. Trentham, D. W. Yates, and R. S. Goody. 1972. Transient kinetic studies of the Mg^{++}-dependent ATPase of myosin and its proteolytic subfragments. *Cold Spring Harbor Symp. Quant. Biol.* 37:127–135.

Brenner, B. 1990. Muscle mechanics and biochemical kinetics. *In* Molecular Mechanisms in Muscle Contraction. J. M. Squire, editor. CRC Press, Boca Raton, FL. 77–149.

Brenner, B., L. C. Yu, and J. M. Chalovich. 1991. Parallel inhibition of active force and relaxed fiber stiffness in skeletal muscle by caldesmon: implications for the pathway to force generation. *Proc. Natl. Acad. Sci. USA.* 88:5739–5743.

Cecchi, G., P. J. Griffiths, and S. Taylor. 1982. Muscular contraction: kinetics of cross-bridge attachment studied by high-frequency stiffness measurements. *Science (Wash. DC).* 217:70–72.

Cooke, R., and E. Pate. 1985. The effects of ADP and phosphate on the contraction of muscle fibers. *Biophys. J.* 48:789–798.

Dantzig, J. A., J. W. Walker, D. R. Trentham, and Y. E. Goldman. 1988. Relaxation of muscle fibers with adenosine 5′-[γ-thio]triphosphate (ATP-[γS]) and by laser photolysis of caged ATP[γS]: evidence for Ca^{2+}-dependent affinity of rapidly detaching zero-force cross-bridges. *Proc. Natl. Acad. Sci. USA.* 85:6716–6720.

Dantzig, J. A., Y. E. Goldman, N. C. Millar, J. Lacktis, and E. Homsher. 1992. Reversal of the cross-bridge force-generating transition by photogeneration of phosphate in rabbit psoas muscle fibers. *J. Physiol. (Lond.).* 451:247–278.

Eisenberg, E., and L. E. Greene. 1980. The relation of muscle biochemistry to muscle physiology. *Annu. Rev. Physiol.* 42:293–309.

Ford, L. E., A. F. Huxley, and R. M. Simmons. 1986. Tension transients during the rise of tetanic tension in frog muscle fibers. *J. Physiol. (Lond.).* 372:595–609.

Fortune, N. S., M. A. Geeves, and K. W. Ranatunga. 1991. Tension responses to rapid pressure release in glycerinated rabbit muscle fibers. *Proc. Natl. Acad. Sci. USA.* 88:7323–7327.

Geeves, M. A., R. S. Goody, and H. Gutfreund. 1984. Kinetics of acto-S1 interaction as a guide to a model for the cross-bridge cycle. *J. Muscle Res. Cell Motil.* 5:351–361.

Gillis, J. M., and G. Maréchal. 1974. The incorporation of radioactive phosphate into ATP in glycerinated fibers stretched or released during contraction. *J. Mechanochem. Cell Motil.* 3:55–68.

Godt, R. E., and T. M. Nosek. 1989. Changes of intracellular milieu with fatigue or hypoxia depress contraction of skinned rabbit skeletal and cardiac muscle. *J. Physiol. (Lond.)* 412:155–180.

Goldman, Y. E., M. G. Hibberd, and D. R. Trentham. 1984a. Relaxation of rabbit psoas muscle fibres from rigor by photochemical generation of adenosine-5′-triphosphate. *J. Physiol. (Lond.).* 354:577–604.

Goldman, Y. E., M. G. Hibberd, and D. R. Trentham. 1984b. Initiation of active contraction by photogeneration of adenosine-5′-triphosphate in rabbit psoas muscle fibres. *J. Physiol. (Lond.).* 354:605–24.

Goody, R. S., and H. G. Mannherz. 1975. *In* Protein-Ligand Interactions. H. Sund, and G. Blauer, editors. de Gruyter, Berlin. 109–127.

Greene, L. E., and E. Eisenberg. 1980. Cooperative binding of myosin subfragment-1 to the actin-troponin-tropomyosin complex. *Proc. Natl. Acad. Sci. USA.* 77:2616–2620.

Hammes, G. G. 1968. Relaxation spectrometry of biological systems. *Adv. Protein Chem.* 23: 1–57.

Heinl, P., H. J. Kuhn, and J. C. Rüegg. 1974. Tension responses to quick length changes of glycerinated skeletal muscle fibres from the frog and tortoise. *J. Physiol. (Lond.).* 237:243–258.

Hibberd, M. G., M. R. Webb, Y. Goldman, and D. R. Trentham. 1985. Oxygen exchange between phosphate and water accompanies calcium-regulated ATPase activity of skinned fibers from rabbit skeletal muscle. *J. Biol. Chem.* 260:3496–3500.

Huxley, A. F. 1957. Muscle structure and theories of contraction. *Prog. Biophys. Biophys. Chem.* 7:255–318.

Huxley, A. F. 1980. Reflections on Muscle. Princeton University Press, Princeton, NJ.

Huxley, A. F., and R. M. Simmons. 1971. Proposed mechanism of force generation in striated muscle. *Nature (Lond.).* 233:533–538.

Kawai, M. 1982. Correlation between exponential processes and cross-bridge kinetics. *In* Basic Biology of Muscles: A Comparative Approach. B. M. Twarog, R. J. C. Levine, and M. M. Dewey, editors. Raven Press, New York. 109–130.

Kawai, M., and P. W. Brandt. 1976. Two rigor states in skinned crayfish single muscle fibers. *J. Gen. Physiol.* 68:267–280.

Kawai, M., and P. W. Brandt. 1980. Sinusoidal analysis: a high resolution method for correlating biochemical reactions with physiological processes in activated skeletal muscles of rabbit, frog and crayfish. *J. Muscle Res. Cell Motil.* 1:279–303.

Kawai, M., and H. R. Halvorson. 1989. Role of MgATP and MgADP in the crossbridge kinetics in chemically skinned rabbit psoas fibers. Study of a fast exponential process (C). *Biophys. J.* 55:595–603.

Kawai, M., and H. R. Halvorson. 1991. Two step mechanism of phosphate release and the mechanism of force generation in chemically skinned fibers of rabbit psoas muscle. *Biophys. J.* 59:329–342.

Kawai, M., and Y. Zhao. 1992. Tension/cross-bridge state deduced from sinusoidal analysis. *Biophys. J.* 61:292*a*. (Abstr.)

Kuhn, H. J. 1977. Reversible transformation of mechanical work into chemical free energy by stretch-dependent binding of AMPPNP in glycerinated fibrillar muscle fibres. *In* Insect Flight Muscle. R. T. Tregear, editor. Elsevier/North Holland Biomedical Press, Amsterdam. 307–315.

Lymn, R. W., and E. W. Taylor. 1971. Mechanism of adenosine triphosphate hydrolysis by actomyosin. *Biochemistry.* 10:4617–4624.

Machin, K. E., and J. W. S. Pringle. 1960. The physiology of insect fibrillar muscle. III. The effect of sinusoidal changes of length on a beetle flight muscle. *Proc. R. Soc. Lond. Ser. B Biol. Sci.* 152:311–330.

Mannherz, H. G. 1970. On the reversibility of the biochemical reactions of muscular contraction during the absorption of negative work. *FEBS Lett.* 10:233–236.

Marston, S. B., R. T. Tregear, C. D. Roger, and M. L. Clarke. 1979. Coupling between the enzymatic site of myosin and the mechanical output of muscle. *J. Mol. Biol.* 128:111–126.

Meyer, R. A., T. R. Brown, and M. J. Kushmerick. 1985. Phosphorus nuclear magnetic resonance of fast- and slow-twitch muscle. *Am. J. Physiol.* 248: C279-C287.

Millar, N. C., and E. Homsher. 1990. The effect of phosphate and calcium on force generation in glycerinated rabbit skeletal muscle fibers. *J. Biol. Chem.* 265:20234–20240.

Millar, N. C., and E. Homsher. 1992. Kinetics of force generation and phosphate release in skinned rabbit soleus muscle fibers. *Am. J. Physiol.* 252 (Cell Physiol. 31):C1239-C1245.

Natori, R. 1954. The property and contraction process of isolated myofibrils. *Jikeikai Med. J.* 1:119–126.

Pate, E., and R. Cooke. 1989. Addition of phosphate to active muscle fibers probes actomyosin states within the power stroke. *Pfluegers Arch. Eur. J. Physiol.* 414:73–81.

Saeki, Y., M. Kawai, and Y. Zhao. 1991. Comparison of cross-bridge dynamics between intact and skinned myocardium from ferret right ventricles. *Circ. Res.* 68:772–781.

Schoenberg, M. 1988. Characterization of the myosin adenosine triphosphate (M·ATP) crossbridge in rabbit and frog skeletal muscle fibers. *Biophys. J.* 54:135–148.

Sleep, J., C. Herrmann, T. Barman, and F. Travers. 1992. Inhibition of ATP binding to myofibrils by caged-ATP. *Alpbach Conference on Muscle* (Abstr).

Stein, L. A., R. P. Schwartz, Jr., P. B. Chock, and E. Eisenberg. 1979. Mechanism of actomyosin adenosine triphosphatase. Evidence that adenosine 5′-triphosphate hydrolysis can occur without dissociation of the actomyosin complex. *Biochemistry.*18:3895–3909.

Tawada, K., and M. Kawai. 1990. Covalent cross-linking of single fibers from rabbit psoas increases oscillatory power. *Biophys. J.* 57:643–647.

Taylor, E. W. 1979. Mechanism of actomyosin ATPase and the problem of muscle contraction. *CRC Crit. Rev. Biochem.* 6:103–164.

Tonomura, Y., H. Nakamura, N. Kinoshita, H. Onish, and M. Shigekawa. 1969. The pre-steady state of the myosin-adenosine triphosphate system. X. The reaction mechanism of the myosin-ATP system and a molecular mechanism of muscle contraction. *J. Biochem. (Tokyo).* 66:599–618.

Trybus, K. M., and E. W. Taylor. 1982. Transient kinetics of adenosine 5′-diphosphate and adenosine 5′-(β,γ-imidotriphosphate) binding to subfragment 1 and actosubfragment 1. *Biochemistry.* 21:1284–1294.

Ulbrich, M., and J. C. Rüegg. 1971. Stretch induced formation of ATP-^{32}P in glycerinated fibres of insect flight muscle. *Experientia (Basel).* 27: 45–46.

Walker, J. W., Z. Lu, and R. L. Moss. 1992. Effects of Ca^{2+} on the kinetics of phosphate release in skeletal muscle. *J. Biol. Chem.* 267:2459–2466.

White, H. D., and E. W. Taylor. 1976. Energetics and mechanism of actomyosin adenosine triphosphate. *Biochemistry.* 15:5818–5826.

Zhao, Y., and M. Kawai. 1993. The effect of lattice spacing change on cross-bridge kinetics in chemically skinned rabbit psoas muscle fibers. II. Elementary steps affected by the spacing change. *Biophys. J.* 64:197–210.